Modelling of a Thermal Time-of-Flight Sensor for Low Rate Open Channel Flow

C. Panhans[1*], T. Koch[2], I. Kuehne[3], S. Leonhard[1], R. Hilliges[1], R. Stolle[1] and A. Frey[1]
[1] University of Applied Sciences, Augsburg, Germany
[2] COMSOL Multiphysics GmbH, Goettingen, Germany
[3] Heilbronn University of Applied Sciences, Kuenzelsau, Germany
*Corresponding author: University of Applied Sciences Augsburg, An der Hochschule 1, 86161 Augsburg, christian.panhans@hs-augsburg.de

Abstract: In this study, a simulation of a novel flowmeter used for low rate open channel flows is presented. The design is based on a thermal time-of-flight (TTOF), measurement setup integrated into the bottom pipe wall. The velocity profile of an open channel flow, as well as the thermal inertia of the heat and sensor elements are considered. Results of 3D transient simulations for velocities from 0.03 m/s up to 0.55 m/s are reviewed and assessed. This insight into the flow velocity distribution and temperature distribution allows for optimization of the flowmeter design. Simulation data is compared to measurements of a prototype. A suitable relation between TTOF time shift and mean flow velocity is established.

Keywords: Thermal Time-of-Flight (TTOF), open channel, low rate flow, laminar flow, heat transfer in fluids

1. Introduction

Water transport in the public sewer system is often based on open channel flows, e.g. in a DN100 drainage pipe. Many established methods of measuring flow rates require a fully filled pipe. Flowmeters of this kind could only be used in an open channel by narrowing the pipe diameter to dam the fluid. Other sensors, such as under water ultrasonic flow sensors or above the liquid surface mounted radar based sensors, require a high minimum liquid level or a large installation space, compared to the pipe diameter. Especially for low flow rates of less than 10 mL/s and with water levels of less than 4 mm, only few flow sensors are available. In order to enable the measuring of very low flows, a novel measurement method was developed. The principle of TTOF (thermal time-of-flight) measurement is used.

The heating element and the temperature sensors, the latter implemented as NTC-sensors (negative temperature coefficient), are integrated into the bottom area of the channel wall (cf. Fig 2 in 2.1). The sensors are located downstream and measure the time difference of the passing heat cloud induced by the heat element (cf. Fig. 1).

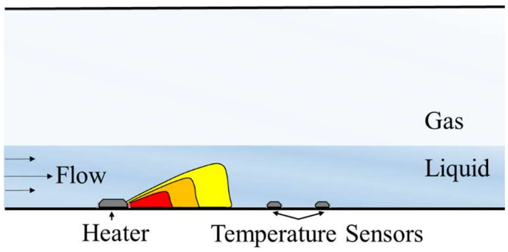

Figure 1. Principle measurement setup of a TTOF flow sensor in an open channel.

TTOF-simulations for fully filled pipe flows are reported in [1]. This work considers low rate open channel flow, which means that the flowing liquid (e. g. water) is measured on the bottom of the pipe, whereas the top is filled with gas (e.g. air). This condition requires a flowmeter design and a modelling approach, which differs from standard TTOF flow measurement of fully filled pipes.

The heater and temperature sensors must be placed at the bottom of the pipe wall, instead of a central position within the pipe, as the fluid level is variable with values down to some hundred micrometers. Having the sensors at the wall with zero flow, the diffusive heat transport orthogonal to the advective heat transport is essential. The main purpose of the presented simulation model is to provide a more detailed qualitative insight to the TTOF functionality under this situation.

While the steady state flow profile can be calculated analytically for the fully filled pipe flow, this is not possible for the velocity profile in a partially filled pipe. Depending on the geometry and flow rate, forces at the liquid-air interface may be relevant. In the model described in this work, such effects can be taken into account by means of an effective friction force.

2. Simulation Model

2.1 Geometry

Using the symmetry of the channel flow results in the 3D model geometry shown in Fig. 2. The heater and the temperature NTC-sensors are modeled as 2D boundaries (cf. section 2.3.1).

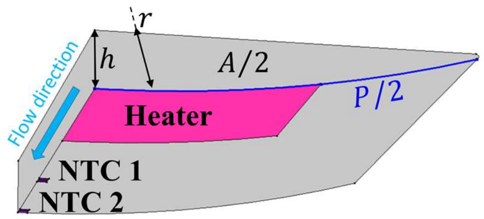

Figure 2. Model geometry (view from below). Meaning of symbols are summarized in Tab. 1.

Table 1: Geometry parameters (cf. also Fig. 2)

Symbol	*Meaning*	*Value*
r	Pipe radius	$50.0\ mm$
h	Water level	$2.1\ mm$
A	Cross-section area	$40.3\ mm^2$
P	Wetted perimeter	$29.1\ mm$

2.2 Governing Equations

2.2.1 Fluid Flow

With the hydraulic raduis r_h defined as [2]:

$$r_h = \frac{A}{P}, \quad (1)$$

the Reynolds number Re for the open channel situation in Fig. 2 can be calculated [2] according to

$$Re = 4v_m \frac{\rho}{\mu} r_h, \quad (2)$$

with density ρ and dynamic viscosity μ of water. A mean velocity range $v_m = 0.28 \ldots 548\ \ \mathrm{mm/s}$ results in $Re = 1 \ldots 2000$. Therfore, the laminar flow is assumed in the flow rates relevant for this work.

The Navier-Stokes equation with the dependent variables velocity field $\boldsymbol{u}$ and pressure p,

$$\rho\left(\frac{\partial \boldsymbol{u}}{\partial t} + (\boldsymbol{u}\cdot\boldsymbol{\nabla})\boldsymbol{u}\right) = -\boldsymbol{\nabla}p + \cdots$$
$$+\boldsymbol{\nabla}\cdot\left[\mu\left(\boldsymbol{\nabla}\boldsymbol{u} + (\boldsymbol{\nabla}\boldsymbol{u})^{\mathrm{T}} - \tfrac{2}{3}(\boldsymbol{\nabla}\cdot\boldsymbol{u})\mathbf{I}\right)\right] + \boldsymbol{F}, \quad (3)$$

together with the continuity equation

$$\frac{\partial \rho}{\partial t} + \boldsymbol{\nabla}\cdot(\rho\boldsymbol{u}) = 0 \quad (4)$$

have to be solved. The material parameters required according to Eq. (3) and (4) are summarized in Tab. 2.

Table 2: Material parameters for liquid water with values taken from [3].

Symbol	*Meaning*
ρ	Density
μ	Dynamic viscosity
C_p	Heat capacity at constant pressure
k	Thermal conductivity

2.2.2 Heat Transfer

The heat injected from the power resistor gets propagated in the channel. The corresponding equation for the dependent variable temperature T

$$\rho\, C_p\left(\frac{\partial T}{\partial t} + \boldsymbol{u}\cdot\boldsymbol{\nabla}T\right) - \boldsymbol{\nabla}\cdot k\boldsymbol{\nabla}T = Q \quad (5)$$

has to be solved. The material parameters in Eq (2) are listed in Tab. 2.

2.3 COMSOL® Implementation

Setup and coupling of Eq. (1) – (3) is easily done by using the COMSOL® *Nonisothermal Laminar Flow* Multiphysics interface in 3D. A *Global ODEs* interface is added to effectively model the thermal inertia of the heater and the NTC-sensors.

2.3.1 Boundary Conditions

According to Fig. 1, a symmetry boundary condition (BC) is used for both, the laminar flow and the heat transfer.
Regarding Laminar Flow, the *Inlet* BC is set to a pre-calculated velocity-profile and the *Outlet* BC is set to *Pressure*. In order to account for the friction at the liquid-gas interface, the according

boundary is set to a *Wall* BC configured with a *Navier Slip* condition [4]:

$$\boldsymbol{u} \cdot \boldsymbol{n}_{surface} = 0 \qquad (6)$$

where $\boldsymbol{n}_{surface}$ is the boundary normal pointing out of the surface. This BC enforces no-penetration at the free liquid surface and furthermore introduces a friction force of the form [4]:

$$\boldsymbol{F}_{fr} = -\frac{\mu}{\beta}\boldsymbol{u} \qquad (7)$$

where β is a *slip length* parameter. It should be pointed out, that using the *Navier Slip* condition is a crude approximation to reality. To get a more precise description, an extensive 3D two-phase turbulent flow simulation could be performed. Because this work is primarily concerned with qualitative modeling, the numerical effort was not justified here.

Regarding Heat Transfer, a *Boundary Heat Source* is inserted. A local *Interpolation function* is used to import measured, time resolved power data $P_{meas}(t)$ at the heat resistance. In order to account for thermal inertia, this data is shaped with the following first order ODE

$$\tau_{heat}\frac{d}{dt}P_{heat\_S} + P_{heat\_S} = P_{meas}(t)\ , \qquad (8)$$

with a characteristic time constant τ_{heat}. The COMSOL® implementation of the ODE is shown in Fig. 3.

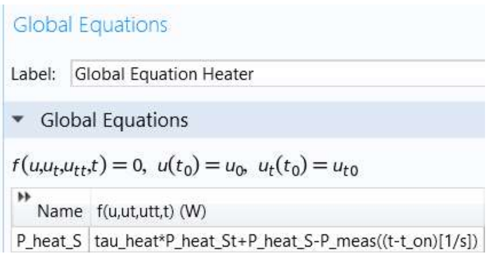

Figure 3. COMSOL® implementation of the ODE for thermal inertia of the heater.

2.3.2 Model Components and Solver Sequence

In order to minimize computational time, the modeled channel length should be limited as much as possible. Fig. 2 shows the minimized channel length defined by the position of the heater at the inlet (begin) and the last downstream NTC-sensors (end). However, to obtain meaningful results in this truncated geometry a well-established flow profile at the inlet is required. To calculate the profile, the following strategy is used: A *Component 1* is setup with *Laminar Flow*, only (cf. Fig. 4), and with a channel length much longer than the minimized one. Furthermore, the *Inlet* BC is set to *fully developed flow*, here. The resulting outflow profile obtained from a first stationary study step (*Step1* in Fig. 4) is transferred to the *Inlet* BC of the final geometry in *Component 2* with a *Linear Extrusion* operator (cf. in Fig. 4 *Component 1: Definitions*). A second stationary study step (cf. *Step2* in Fig. 4) for *Nonisothermal Laminar Flow* in *Component 2* (with minimized channel length) is used to calculate initial conditions for the transient simulation performed in a third study step (cf. *Step3* in Fig. 4). Details of the *Study* configurations for *Step 3* are shown in Fig. 5.

The reported model setup also allows for a *Parametric Sweep* of systems parameters.

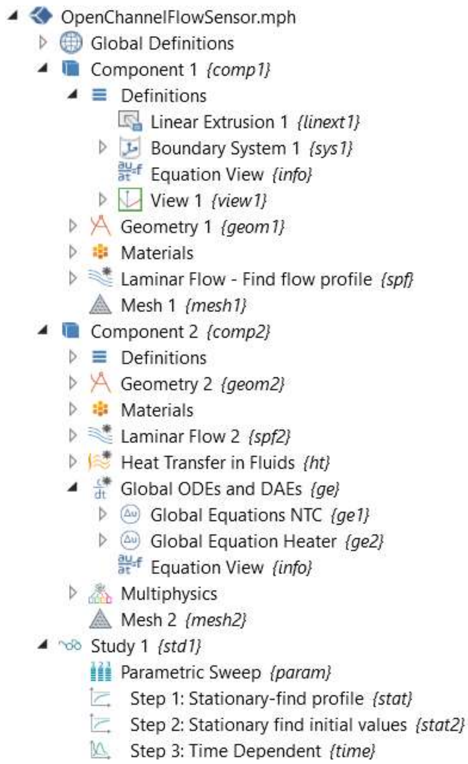

Figure 4. Model Builder.

The temperature field over each NTC-sensor boundary is averaged to $\overline{T}_{NTC}$ with a *Component Coupling* operator. Taking the thermal inertia of the NTCs into account, global ordinary differential equations (ODE) of the form given in Eq. 9 are added to *Component 2* with a characteristic time constant τ_{NTC} obtained from experimental data. The NTC temperature signal T_{NTC_S} is fed into the signal processing electronics as follows:

$$\tau_{NTC} \frac{d}{dt} T_{NTC\_S} + T_{NTC\_S} = \overline{T}_{NTC}(t) \qquad (9)$$

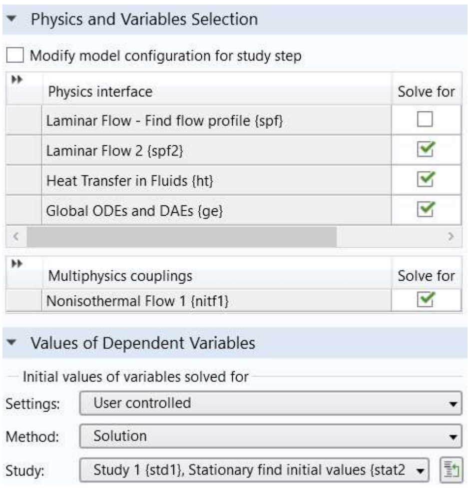

Figure 5. Details of the *Study* configurations for *Step 3: Time Dependent* (also cf. Fig. 4).

3. Results

3.1 Simulations

Fig. 6 shows typical results for the open channel flow profiles.

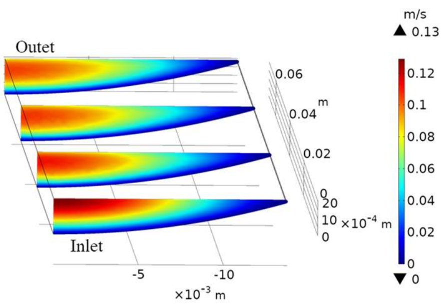

Figure 6. Velocity of the fluid at mean velocity $v_m = 0.06$ m/s in several cross sections of *Step 1: Stationary find profile*.

In Fig.7, the velocity-profiles at the in- and outlet, obtained from the *Step 1* study step, are compared. The left part of the graphs represent the velocity over the length of the horizontal cut line whereas the right side represent the velocity over the length of the vertical cut line. While the velocity at the pipe wall is zero, it reaches the maximum at the center of the cross section, beneath the fluid surface.

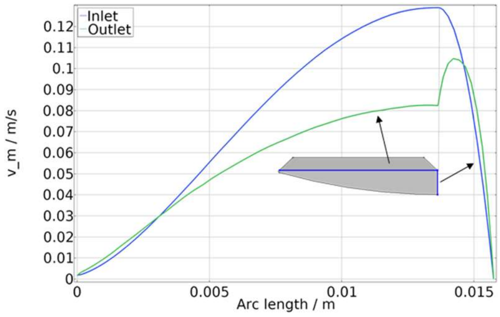

Figure 7. Comparison of inlet and outlet velocity at mean velocity $v_m = 0.06$ m/s of *Step 1: Stationary find profile*.

For the results of *Step 3: Time Dependent*, the heat distribution over the vertical cut plane along the center of the pipe is evaluated. As shown in Fig. 8, the heat cloud rises during the pulse time from 0.10 s to 0.35 s and is moving downstream. The distortion of the heat cloud due to the flow profile is responsible for the flatness. With rising flow velocity, the flatness and the distribution of the heat cloud rises, which results into a decreasing measurable temperature amplitude at the NTCs.

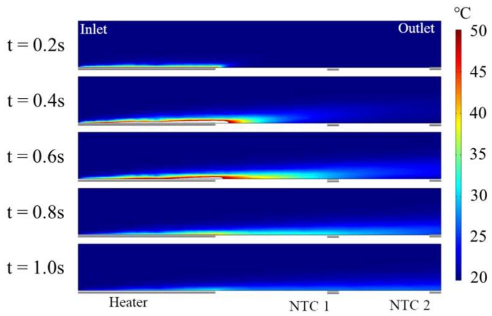

Figure 8. Temperature distribution of vertical cut plane for several time steps at mean velocity $v_m = 0.06$ m/s.

The average temperatures of the NTC boundaries over time are approximately shaped as a low-pass-filtered rectangular pulse, as illustrated in

Fig. 9. The curve of NTC 2 is about half of the amplitude of the one of NTC 1, while the peaks are 30 ms time shifted at $v_m = 0.06$ m/s.
The temperature peak of NTC 1 in Figure 9 appears a short time interval before the moment when the core of the heat cloud passes NTC 1.

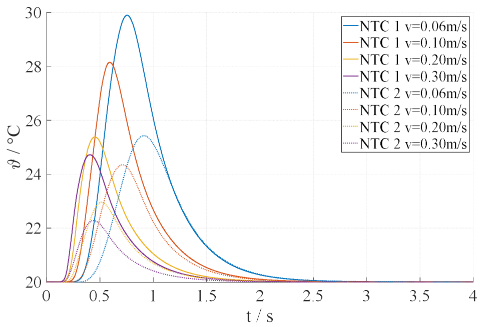

Figure 9. Temperature over time at NTC 1 and NTC 2 for several mean flow velocities.

The ODEs, modeling the thermal inertia of the sensors act as a low-pass-filter to the temperature curves, causing a decrease in amplitude and an increase in time shift of the calculated NTC temperature response (cf. Fig. 10).

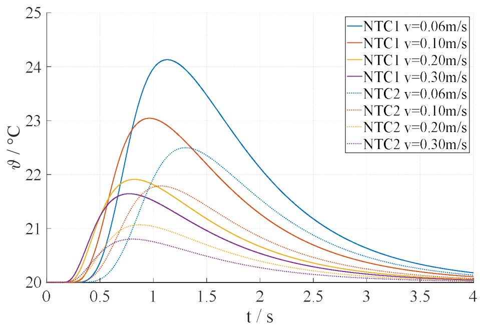

Figure 10. Thermal inertia considered temperature response over time at NTC 1 and NTC 2 for several mean flow velocities.

Both, the peak of the temperature pulse at the surface and the peak temperature of the NTCs including the ODEs are decreasing as the flow velocity rises (cf. Fig. 11).

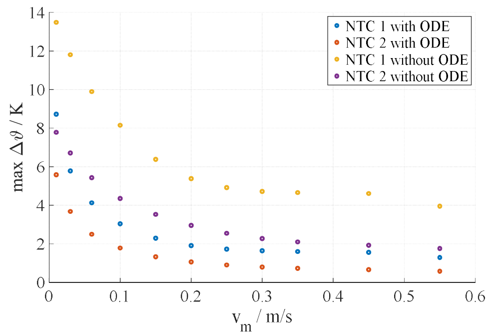

Figure 11. Maximum temperature at NTC 1 and NTC 2 for several mean flow velocities.

The TTOF measurement principal is using the time shift as input information for the calculation of input velocity, e.g. from peak to peak. For standard TTOF as reportet in [5], the velocity is linearly dependent from the time shift and the distane between temperature sensors. However, the simulation results for the investigated TTOF scheme show a non-linear dependency between the flow rate and the time shift as shown in Fig. 12. A curve is fitted to the simulated data points by the help of the function

$$\Delta t = a v_m{}^n \qquad (10)$$

with the two fitting parameters a and n. Fitting the data without ODEs results in the parameters a = 0.0135 and n = −0.8842, and for data with considered thermal inertia of the NTC-sensors a = 0.01275 and n = −0.9042.

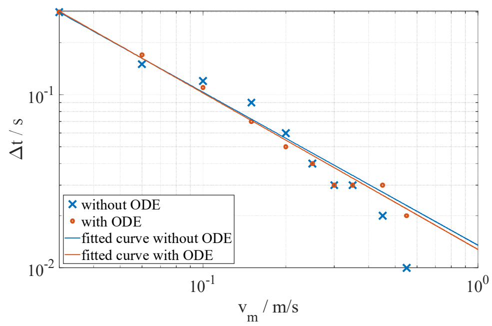

Figure 12. Peak-to-peak time shift over flow velocity, with and without NTC-ODEs.

3.2 Experimental Work

A TTOF flowmeter prototype is utilized to compare the simulation results to experimental data. The heat element, made of SMD resistors of chip type 2512, and the NTC-sensors with the B-parameter 3950 are taped to the bottom of a 100 mm pipe made of polyvinyl chloride (PVC). Both, wires to the heating element as well as the wires to the NTCs are shielded with copper tape and routed separately to obtain sufficient electromagnetic shielding. The elements are covered with a thin layer of waterprotective coating. All dimensions of the prototype match the ones used for the COMSOL® simulation. Due to surface tension, the water covered arc length varies along the pipe (cf. Fig. 13).

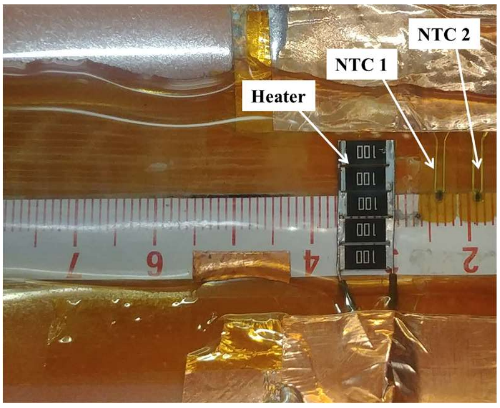

Figure 13. Top view of the TTOF open channel prototype during measurement.

Fig. 11 shows that the NTC temperature rise is only a few Kelvin. The electronics converting the temperatures to voltages suitable for standard analog-to-digital-converters consist of amplifiers, which behave as a differentiator. This reshapes the signal significantly and causes undershoot as displayed in Fig. 14.

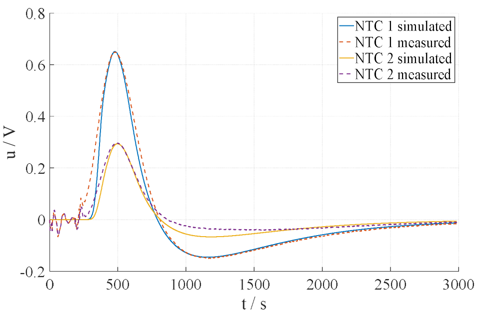

Figure 14 Comparison of simulation and measurement data.

The simulated NTC temperature signals are converted to measurement equivalent voltages with a Simulink signal path model. However, the absolut time difference and the amplitudes of the simulation based voltage signals do not match the measurement results. Nevertheless, by adjusting these voltages in amplitude and absolute time shift provides reasonable agreement of the pulse shape and peak-to-peak time shift between simulation and measurement results (cf. Fig. 14).

4. Conclusions

In this work, a simulation model of an innovative TTOF open channel flowmeter is presented. It is based on the *Nonisothermal Laminar Flow* Multiphysics interface coupling *Single-Phase Flow* and *Heat Transfer*. The velocity profile results from a *No Slip* BC at the pipe wall and a *Navier Slip* BC for the fluid-gas surface.

In order to optimize computation time, the model is built of two components. One is used to calculate the steady state flow profile. The other is utilized for the transient simulation. The model allows for parametric sweeps and is organized in three study steps.

The presented TTOF flowmeter simulation model provides insight into the measurement principle. Fundamental differences to fully filled pipe flow [1, 5] become apparent.

The heat cloud dissolves while streaming down the flow in such a way that the heat core, which passes the NTC-sensors has a lower temperature than the envelope of the heat cloud, which passed the NTC-sensors beforehand. This effect is reinforced by the fact, that the temperature sensor can not be placed in a central position of the lamiar flow.

Overall, this leads to a non-linear relation between peak-to-peak time shift and mean velocity. However, the deviation of the time shift from the fitted curve increases with rising mean velocity, due to the finite temporal resolution of the simulation.

Another insight of the model is that only the bottom layers of the open channel are involved in the heat transport, especially for higher flow velocities. Moreover, it becomes apparent that minimizing the thermal time constants of the heat and sensor elements is essential to improve the sensitivity of the measurement setup.

A next step in future work is an improved TTOF prototype with lower mechanical tolerances and less signal distortion caused by the amplifier circuit. Thereby, a quantative comparison of measured and simulated values for different environmental parameters, such as water level and fluid base temperature, seems possible.

References

[1] Ecin, O. et all: Modelling Thermal Time-of-Flight Sensor for Flow Velocity Measurement, Proceedings of the COMSOL® Conference 2009.

[2] Robert Freimann, *Hydraulik für Bauingenieure. Grundlagen und Anwendungen.*, Carl-Hanser-Verlag, München 2009.

[3] COMSOL® Material Library

[4] COMSOL® CFD Module Users Guide

[5] Engelien, E. et all: Evaluation on Thermocouples for the Thermal Time-of-Flight Flow Measurement, *54th IWK* Ilmenau (2009).